^{3}He(π^-,π^0) reaction at T_π=200 MeV

M. D. Cooper, H. W. Baer, J. D. Bowman, F. H. Cverna, R. H. Heffner, C. M. Hoffman, N. S. P. King, and J. Piffaretti*
Los Alamos National Laboratory, Los Alamos, New Mexico 87545

J. Alster, A. Doron, S. Gilad,† and M. A. Moinester
Tel Aviv University, Ramat-Aviv, Israel

P. R. Bevington‡ and E. Winklemann§
Case Western Reserve University, Cleveland, Ohio 44106
(Received 8 June 1981)

Energy and angle differential cross sections for the ^{3}He(π^-,π^0) reaction at T_π=200 MeV have been measured. Angular distributions for the isobaric analog state and the energy integrated continuum have been obtained from 0° to 90°. The excitation of the analog state seems to be best represented by Glauber model calculations with nuclear wave functions suitable to explain electron scattering, but all model calculations underestimate the forward angles by 1.5 standard errors. The continuum angular distribution has the same shape as the free $p(\pi^-,\pi^0)n$ reaction except at forward angles, where the cross section is suppressed by Pauli blocking of the final state. The total isobaric analog state cross section is 6.29±0.94 mb and the total charge exchange cross section from 0° to 90° is 28.4±3.8 mb. The latter is one-half the plane wave impulse approximation value.

[NUCLEAR REACTIONS ^{3}He(π^-,π^0); T_{π^-}=200 MeV; measured $\sigma(\theta)$; θ=0°–90°; analog state; continuum; compare to theory; deduced effective number of nucleons and Pauli blocking effects.]

I. INTRODUCTION

The opportunity exists in pion nuclear physics to illuminate the character of the pion-nucleus optical potential by a set of carefully chosen experiments. The situation is analogous to the nucleon-nuclear potential where nucleon charge exchange played a key role in understanding the isospin-dependent piece of the potential. In pion-nucleus scattering, the isospin-dependence is richer because the isovector nature of the pion produces more open channels that need to be studied for a complete description of the potential. The list of experiments necessary to characterize the isospin dependence of the pion-nucleus optical potential includes the measurement of total cross sections, elastic scattering with both positive and negative pions, single-charge exchange, and double-charge exchange. This paper concerns the single-charge exchange aspect of the problem via the isobaric analog state transition.

Optical potentials used to describe scattering are expressed typically in terms of many variables, but the common parameters are usually the target mass and the projectile energy. In mapping the mass dependence of the potential, the few-nucleon problem has played an intermediate role between nucleon-nucleon scattering and the complete many-body problem. The few-nucleon problem has the advantage that fewer assumptions are necessary to explain the data than for high mass nuclei because the full complexity of n-particle interaction does not enter the calculations. For example, multiple scattering expansions can be summed for small n. Hence, it should be a prerequisite for a successful theory of pion charge exchange that it make accurate predictions for the analog transition in ^{3}He(π^-,π^0)^{3}H.

In nuclei lighter than ^{7}Li, there is only one isobaric analog transition available, that which carries ^{3}He into ^{3}H or *vice versa*. Studying the ^{3}He(π^-,π^0) reaction is particularly favorable in that there is only one state of ^{3}H and it is bound by 6.2 MeV. This fact allows a clean experimental

separation of the isobaric analog state from the continuum charge exchange scattering using the high resolution available from the new LAMPF π^0 spectrometer.[1] The ^{3}He(π^-,π^0) measurement was performed for several reasons. In addition to those above, the analog state reaction on ^{3}He has been the subject of detailed theoretical calculations. These calculations have used three approaches: the Glauber model,[2] the coupled channels optical model,[3] and the multiple scattering approach.[4] These approaches make the same qualitative prediction: The angular distribution of the isobaric analog state will be rather featureless because it is the sum of two terms that complement each other's structure. These terms are the spin-flip and nonspin-flip amplitudes. However, these reaction models predict different magnitudes and shapes for the cross sections. The purpose of this experiment is to measure the angular distribution to see if the data favor any of the calculations.

This experiment will also measure the continuum charge exchange region. The π^0 spectrometer will allow measurement of the continuum to nearly 0°. No detailed theoretical work exists on the shapes of the continuum spectra. The dominant quasifree single-charge exchange is expected to be influenced by Pauli blocking, two- and three-body breakup, and final state interactions.[5]

Experimentally, the situation is one of very little data. Continuum data on heavy nuclei were obtained by Bowles *et al.*,[6] and radiochemical methods have been used to study total cross sections to a few bound states.[7] In the mass three system, the recoiling nuclei were detected in experiments[8,9] performed between T_π=133 and 290 MeV. These have yielded data over part of the backward scattering hemisphere which are interesting but insufficient to identify the dominant characteristics of the reaction mechanism. Recently, measurements using the π^0 spectrometer have been reported for analog state charge exchange on a variety of nuclei near 0°.[10]

This paper reports the first complete angular distribution information on pion single charge exchange from nuclei. The energy T_π=200 MeV was chosen to be one of those used in the recoil experiment of Källne *et al.*[9] in order to obtain the most complete distribution and to cross check the experiments.

II. EXPERIMENTAL DETAILS

The experiment was performed at the low energy pion channel of the Clinton P. Anderson Meson Physics Facility (LAMPF). The apparatus is illustrated in Fig. 1. The channel was adjusted to

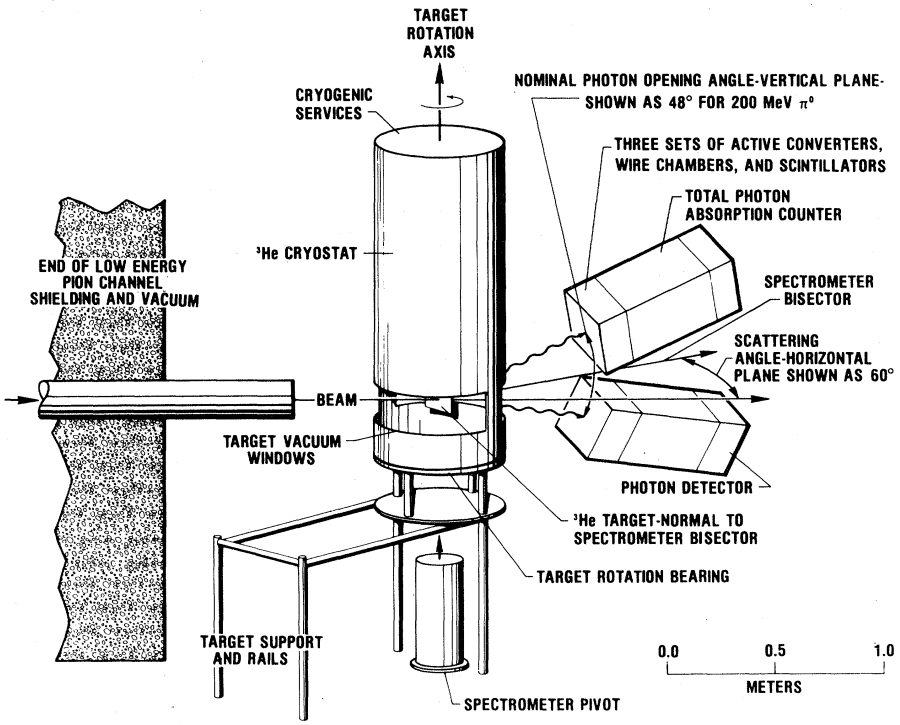

FIG. 1. The experimental layout with the ^{3}He cryogenic target in place. Only a schematic representation of the π^0 spectrometer is shown. A complete description is given in Ref. 1.

select 311-MeV/c negatively charged particles which corresponded to 200-MeV pions. The pion intensity was reduced from the maximum available to prevent pileup in the π^0 spectrometer and to minimize the contribution of the channel's momentum acceptance to the π^0 energy resolution. The flux was 1.0×10^6 pions/s for angles between 0° and 66° and 1.2×10^7 pions/s for angles near 80°. The momentum acceptance of the channel was 1.0% full width and made a 2.4-MeV contribution to the π^0 energy resolution.

A ^{3}He cryogenic target, on loan from the University of Virginia,[11] was modified in two ways. Firstly, a cumbersome vacuum flange, which held the vacuum window through which the beam passed and which would have caused the photons to traverse a third of a radiation length of matter, was replaced by Fiberglas bands and epoxy of inconsequential thickness. Secondly, the target cell was replaced by one 12.5-cm high by 17.6-cm wide by 1.28-cm deep.

Since the target cell windows bulge, the actual target thickness was measured by the method of range difference.[12] The beam was tuned for 45-MeV pions and a stopping distribution for the beam particles for the full target cell was measured in a series of 0.05-cm-thick scintillators. This was compared to the stopping distribution obtained with an empty target cell and a known amount of aluminum sheet in the beam. The aluminum thickness was adjusted to match the two stopping distributions so that the ^{3}He target thickness was the gram thickness of the aluminum corrected for the difference in the stopping powers of Al and ^{3}He. The resulting thickness of ^{3}He was 0.116 g/cm^2. At each scattering angle, the target thickness was corrected for the angle the target made with the beam.

The target was geometrically aligned to lie on the π^0 spectrometer axis of rotation. This positioning preserved the absolute energy calibration of the π^0 spectrometer to about 1 MeV. As the scattering angle changed, the target rotated about its vertical axis so that the target plane was normal to the spectrometer bisector as required for best π^0 energy resolution.[1]

Since the ^{3}He target was symmetric about its vertical axis, a horizontal scattering plane is required for the angular distribution. Thus, the π^0 spectrometer was set up in its one-post configuration.[1] This setup placed the photon detectors symmetrically above and below the scattering plane. The scattering angle was changed by moving both detectors about the target in the horizontal plane. The distance from the target to the first photon converter was 1 m and the angle between the spectrometer arms was 48°, an optimal setting for a 200 MeV π^0.

The data presented in this paper took about 4.5 d to collect. This time was allocated as follows: 3 d on ^{3}He, 0.5 d on CH_2, 0.5 d on background studies, and 0.5 d on target thickness measurements. The spectrometer was set for central laboratory scattering angles of 0°, 20°, 40°, 62°, and 80°. The beam flux was unchanged except for the 80° data. Spectra from CH_2 were taken for all channel settings. Empty target data revealed only a negligible contribution to the spectra from vacuum foils in the beam.

The data were recorded on magnetic tape by a PDP-11/45 computer. Also recorded were radioactive source[13] spectra for each glass element which were used to monitor the stability of the photomultiplier tubes. The data were analyzed with careful monitoring of instrumental stability. Corrections were made for gain drifts in the photomultiplier tubes and efficiency changes in the multiwire proportional counters. Only a small fraction of the raw trigger events appeared in the final spectra. The process for selecting the final events was monitored from angle to angle to ensure that the efficiency for acceptance was stable to 5%.

Since the angular resolution of the spectrometer is substantially smaller than its angular acceptance, the data were divided into two equal angular bins. The angular resolution varies from 4° at $\theta=0°$ to 2° at $\theta=80°$ However, lack of statistics and an expected lack of structure in the angular distribution made finer angular binning inappropriate. For central laboratory scattering angles $\geq 20°$, the acceptance is symmetric about the central angle and triangular. The base of the triangle is $\pm 12°$ wide. This acceptance function produces less than a 2% error in the cross sections if the bin angles are denoted in a way which averages the effects of variations in the cross section across the bin; these angles are $+4°$ and $-4°$ from the central angle for this data set.

The effective solid angle, including efficiency, for the spectrometer was determined from the 0° data on a CH_2 target by comparing the ^{3}He data to the known laboratory cross section[14] for $p(\pi^-,\pi^0)n$ of 12.9 ± 0.65 mb/sr at a scattering angle of 3°. This method of determining the solid angle of the spectrometer agrees to within 20% with an abso-

lute determination involving a Monte Carlo estimate of the geometrical solid angle, a calculation of the photon conversion probability, efficiencies of the detector elements, and event reconstruction efficiencies.[10] The relation between the angular bins in the 0° data on ^{3}He and the 0° data on CH_2 was made by binning the data in the same way for both targets at 3° and 11°. At the larger scattering angles, hydrogen data could not be taken because of background from charge exchange on carbon. As stated for the large angle range, the spectrometer angular acceptance is nearly symmetric about the central angle. Using the fact that the full spectrometer solid angle is independent of the scattering angle, the ^{3}He bins were taken to have half the solid angle of the entire 0° CH_2 data.

Two important corrections to the solid angle are necessary. The first is needed because photons from π^0 decay exiting the ^{3}He target must traverse a 4°K thermal radiation shield, a 70°K thermal radiation shield, and a vacuum jacket; the total material corresponded to 1.57 cm of aluminum for each photon. In the CH_2 data, taken without the cryostat, no such material existed. The pair production cross section in aluminum for 170-MeV photons is a slowly varying function of energy and yields an attenuation length of 15.3 cm. The solid angle is reduced by 23% relative to CH_2 because charged particles are vetoed.

The second correction is due to the energy acceptance of the spectrometer. The energy acceptance enters both in obtaining the shape of the continuum spectrum and in extracting the analog angular distribution. It affects the analog state cross sections because the light mass of the recoiling tritium causes a 29-MeV range in the energy of the π^0 as a function of π^0 angle. The correction is made by dividing all spectra by the spectrometer acceptance function, assumed to be an asymmetric triangle and based on Monte Carlo computer studies. The top of the triangle was normalized to unity for 200-MeV π^0's and went to zero at 120 and 304 MeV.

The final π^0 spectra are shown in Fig. 2. All the spectra consisted of three components: an isobaric analog transition, continuum charge exchange, and a flat background from charge exchange in the air before and after the target. The background from the air was flat in empty target runs. To separate the components, the background was extrapolated from the kinematically forbidden energy range above the isobaric analog state. The continuum was assumed to be smooth and was taken to rise linearly from its kinematic endpoint, 6.2 MeV above the analog state. The measured continuum can extend to lower excitation energies due to finite energy resolution. The analog state line shape was taken from the $p(\pi^-,\pi^0)n$ measured line shape.

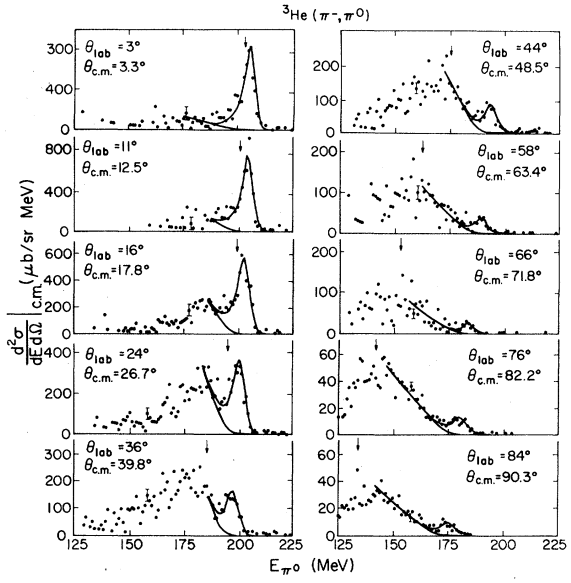

FIG. 2. The double differential cross section for ^{3}He charge exchange is depicted versus energy and angle. A typical statistical error is shown in each panel. The fits to the analog state above the continuum background are shown by the solid curves. The arrow locates the π^0 energy appropriate for the free $p(\pi^-,\pi^0)n$ reaction.

The hydrogen line had a resolution of 5.5 MeV FWHM. This resolution could be accounted for largely by three components: finite momentum spread in the channel (2.4 MeV), spectrometer aberration produced by finite target thickness (2.0 MeV), and intrinsic spectrometer energy resolution (3.5 MeV). A Gaussian of variance σ^2, caused by other uncertain aberrations, could be convoluted with the hydrogen line shape. At 0°, σ was zero. From 20° to 62°, there was a slight statistical preference for σ to be 1 MeV. At 80°, σ was 2 MeV, which can be explained because the target could not be placed normal to the spectrometer bisector as required for optimal resolution.

The decomposition of the spectra into background, continuum, and ground state can be seen from the solid lines in Fig. 2. The solid lines are the total fit to all three components and the continuum plus background contributions. The data were fit by the maximum likelihood method.[15] The likelihood function that was maximized was

$$L = \prod_i e^{-f_i} \frac{f_i^{k_i}}{k_i!} , \quad (1)$$

where i is the channel number in the spectrum, k_i is the number of counts in channel i, and f_i is the predicted number of counts in channel i. The prediction is the sum of the three components with coefficients which are determined by the fitting procedure. Equation (1) is recognized as properly representing the Poisson statistics for a small number of counts per channel. It is necessary to use Eq. (1), as opposed to a least squares procedure, to prevent a biased fit that does not preserve the total number of counts in the spectrum.[16]

The results to be presented in the next section are quoted with absolute errors for integrated cross sections and relative errors for differential cross sections. The absolute errors are obtained from the relative ones by folding in a 10.3% common error. The contributions to the absolute errors are statistics in the $p(\pi^-,\pi^0)n$ spectrum (3%), uncertainties in the $p(\pi^-,\pi^0)n$ cross section (5%), the target thickness (8%), and the photon attenuation in the cryogenic target (3%).

The relative errors are angle dependent. In addition to statistical uncertainties, there are uncertainties arising from the relative flux correction for the 80° data (10%), the finite angular acceptance ($\leq 2\%$), and instrumental stability (5%). For the analog state, the energy acceptance of the spectrometer contributed an error which increased with angle (up to 4%). For the continuum, the error at large angles due to energy acceptance was asymmetric. These errors were bounded from below by the observed counts and from above by the uncertainties in the acceptance (up to 40% at 84°).

III. RESULTS AND DISCUSSION

Figure 2 shows the spectra as a function of π^0 energy and angle. At the largest angles, the continuum cross section falls rapidly near 130 MeV, where the spectrometer acceptance is small. Although the data have been corrected for the variation of the acceptance, there is a substantial uncertainty in the shape of the low-energy parts of the data. In what follows, this uncertainty has been included in the errors by estimating the change in cross section which would result from changing the acceptance function to one with the maximum allowed variation from the standard acceptance function.

The arrows in Fig. 2 locate the π^0 energy corresponding to charge exchange from hydrogen. The deviations of the peaks of the continuum data from the arrows demonstrate how the quasifree scattering is modified by binding, final state interactions, and other nuclear effects.

Aside from the analog state, the continuum π^0 spectra are composed of two- and three-particle final states. An interesting test of any theory of this continuum will be to see whether it can predict the shape of these spectra. In particular, the relative contributions of two- and three-body final states must be estimated properly. The greatest sensitivity of this ratio probably will be in the threshold region just below the analog state peak in π^0 energy. To date, the best attempt at this type of calculation has been done for the electrodisintegration of tritium,[17] but the theoretical predictions have not been quantitatively successful.

The decomposition of the analog state from the continuum according to the procedure of Sec. II is also shown in Fig. 2. At a level much below the statistical uncertainties, the areas of the analog state peaks are insensitive to the details of how the background regions are chosen so long as the kinematic constraints are respected. The change with angle in the energy of the analog state is clearly seen in the spectra and demonstrates that the spectra obey the predicted kinematic shifts.

Figure 3 shows the angular distribution of the analog state including the data from the recoil experiment of Källne *et al.*[9] These data represent the first nearly complete pion charge exchange angular distribution to a discrete state ever measured.

The large-angle π^0 and recoil measurements imply either that the cross section falls very rapidly near 95° or that there are normalization differences between the experiments. There is no way that the quoted errors in this paper can accommodate a factor of 2.0 reduction in the 90° center-of-mass cross section necessary to produce a smooth angular distribution. Future experiments will have to resolve this apparent inconsistency.

Figure 3 shows three theories representing different approaches. The solid line is the Glauber approach of Gerace *et al*,[2] the long-dashed curve is the optical model calculation of Landau,[3] and the short-dashed curve is a Monte Carlo multiple scattering prediction of Hess and Gibson.[4]

All of these theories verify the prediction of Sparrow[18] that there are two important contributions to the analog cross section: direct and spin-

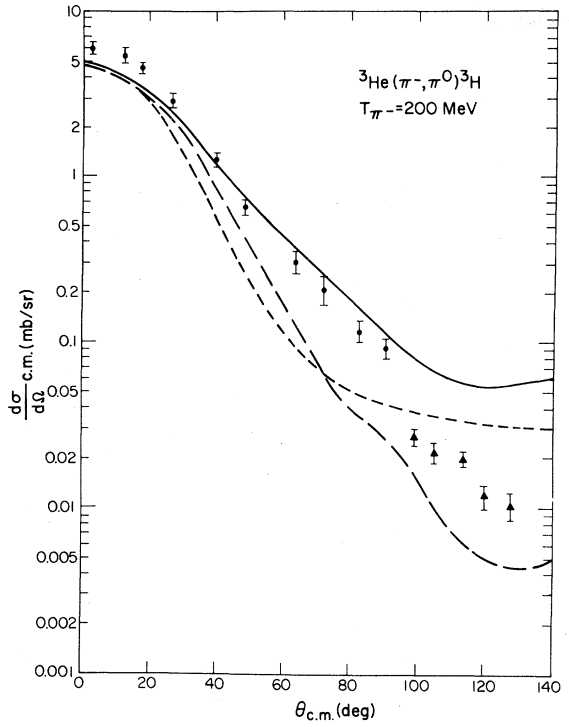

FIG. 3. Angular distribution for ^{3}He(π^-,π^0)^{3}H from the present measurement (circles) and the tritium recoil experiment of Källne *et al.* (Ref. 9) (triangles). An absolute normalization uncertainty must be added in quadrature to the plotted standard deviations for both the present measurement (10%) and that of Källne *et al.* (15%). The curves are Glauber (Ref. 2) (solid), optical potential (Ref. 3) (long dash), and multiple scattering (Ref. 4) (short-dash) calculations.

flip charge exchange. The direct term is expected to have a minimum near 55° due to *s*- and *p*-wave interference in the π-nucleon amplitude. This deep minimum is not observed because the spin-flip contribution peaks near 40°. The sum of these two cross sections produces a rather featureless angular distribution. This result is verified by the data.

The 0° cross section of 6.1±0.8 mb/sr lies between the charge exchange cross sections to isobaric analog states from hydrogen (12 mb/sr at 200 MeV) and the preliminary value[19] from ^{7}Li (4 mb/sr at 180 MeV). All the calculations underestimate the cross section near 0°, but the effect is only 1.5 standard deviations. The three approaches differ substantially in the magnitude they predict for the cross section beyond 30°. In order of agreement with these data, the preferred calculations are the Glauber, optical model, and multiple scattering techniques. The larger Glauber cross section of Gerace *et al.*[2] is reproduced by the Glauber calculations of Lohs and Mandelzweig,[20] though the latter theory falls faster beyond 80°. Though the Glauber calculation comes closer to predicting the present data, it is far inferior to the optical model calculations in predicting π^- elastic scattering[3,21] on ^{3}He at 200 MeV. The good agreement between Glauber calculations and the data may be fortuitous, since the Glauber approximation is a forward angle model and may not be reliable at 90°. Wakamatsu[22] has also calculated the reaction using the optical model and obtains nearly the same results as Landau.[3] One difference is the claim that substantially more cross section at intermediate angles is found by including double spin-flip terms. The effect cannot be quantitatively checked because Wakamatsu's curves are 25% reduced relative to Landau's.

The calculations mentioned above differ only in the number of nucleon scatterings to which the spin-flip and nonspin-flip contributions are calculated and the details of the nuclear wave functions tions used. Gerace *et al.* claim the larger predicted cross section is due to improved wave functions.

The angular distribution in Fig. 3 can be integrated to obtain the total cross section for analog charge exchange from ^{3}He. The result is 6.29±0.94 mb and assumes no consequential contributions beyond 130°. As expected from Fig. 3, this result is in agreement with Gerace *et al.* (6.2 mb), but about 50% larger than the calculations of either Landau (4.8 mb) or Hess and Gibson (4.1 mb).

Integrating the continuum double differential cross sections of Fig. 2 over energy gives the cross section for continuum charge exchange as a function of angle. This angular distribution is plotted in Fig. 4. The solid curve is 1.03 times the free $p(\pi^-,\pi^0)n$ cross section in the ^{3}He center-of-mass system. The cross section tracks the shape of $p(\pi^-,\pi^0)n$ quite closely in the angular region between 40° and 80°. This is the same result as found at larger angles by Bowles *et al.*[6] on heavier targets.

The irregular shape of the continuum angular distribution near 0° is thought to be instrumental, though no quantitative explanation has been found. The dashed curve is a smooth curve through the data which assumes the fluctuation is statistical.

Pauli blocking affects the charge exchange data in two ways. The first is to suppress the quasifree scattering near small angles. For low excitation energies, there is insufficient momentum transfer

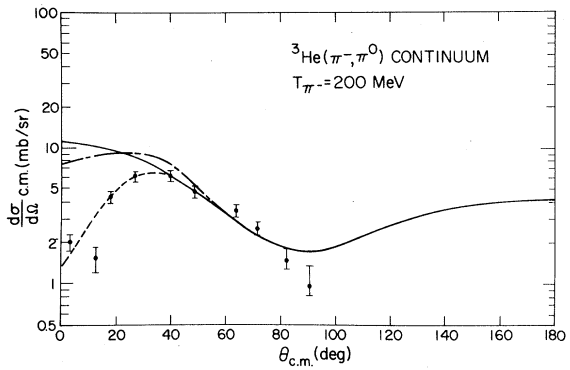

FIG. 4. Angular distributions for continuum charge exchange from ^{3}He. The solid curve is 1.03 times the $p(\pi^-,\pi^0)n$ cross section in the ^{3}He center-of-mass system. The dashed curve goes smoothly through the data, and the dash-dot curve has the analog state cross section added to the dashed curve.

available to make the final state lie above the already occupied momentum states. At high excitations, the momentum matching of the reaction is poor. The Pauli blocking is seen in the data at forward angles, where the cross section is substantially suppressed in Fig. 4 relative to the free π-nucleon cross section. No theory exists for the shape of the inhibition.

The dash-dot curve is the sum of the analog state cross section and the dashed curve and is closer to the shape of the free $p(\pi^-,\pi^0)n$ cross section. Hence, the analog state cross section accounts for about half of the missing cross section in the continuum. The remaining difference has its origin in distortions of the pion scattering and bound nucleon wave function from the plane waves of the free scattering. Additionally, the second effect of Pauli blocking is to prevent population of the bound neutron final state already occupied by the neutron in ^{3}He. The situation is analogous to heavy nuclei, where much of the final nuclear shell may be occupied.

The inhibition of quasifree scattering at forward angles has been observed[23] previously for inelastic scattering of π^+ from ^{16}O at angles larger than 30°, but the missing cross section has not been compared to the scattering to low lying states because a large part of the cross section arises from Coulomb scattering. That the sum of all charge exchange tracks the free nuclear charge exchange angular distribution is known for ^{16}O outside of 25° from the measurements of Bowles *et al.*[6] However, their resolution was not sufficient to separate the discrete states from the broader charge exchange continuum.

The integral of the angular distribution in Fig. 4 is calculated from the dashed curve forward of 40° and the solid curve at backward angles. The total continuum charge exchange cross section over the region from 0° to 90° is 22.1 ± 3.4 mb. There is no direct evidence that the cross section continues to follow the solid curve to 180°, but it is a reasonable assumption in light of the measurements of Bowles *et al.*[6] Under this assumption, the total continuum cross section would be 39.4 mb.

The total charge exchange cross section is obtained by adding the analog state and continuum total cross sections. The result is 45.7 mb and the value in the forward hemisphere is 28.4 ± 3.8. For the range 0° to 90°, the ratio to the free hydrogen cross section is 1.10 ± 0.14. In the absence of flux removal by other channels, the expectation for this ratio is 2 because there are two protons in ^{3}He.

The ratio of the total charge exchange cross section to the nucleon cross section has been dubbed N_{eff} by Ashery *et al.*[24] and Burleson *et al.*[25] Extrapolating their data as a function of charge at 205 MeV to $Z=2$ yields an N_{eff} of 1.20. Considering the experimental errors and rapid energy dependence of N_{eff}, the agreement is quite good. Continuing the extrapolation to $Z=1$ yields an N_{eff} of approximately 0.8. Norem[26] found $N_{\text{eff}}=0.7$ for $d(\pi^+,\pi^0)$ at 182 MeV, not bad agreement with Ashery *et al.* considering the energy difference. Hence, the total charge exchange cross section for ^{3}He at 200 MeV fits the systematics extrapolated from other nuclei.

IV. SUMMARY

This experiment provides the most detailed information available on pion single-charge exchange on one nucleus at one energy. A complete angular distribution for the analog charge exchange has been measured which verifies the importance of spin-flip contributions to pion charge exchange in light nuclei. The data are in good agreement with Glauber model calculations. Double differential cross sections and an energy integrated angular distribution have been obtained for the continuum as well. The continuum angular distribution resembles the free nucleon cross section in the forward hemisphere except for the angular region influenced by Pauli blocking. The measurement of the continuum at very small angles has provided clear evidence for suppression of the cross section. The total cross section for analog charge exchange is

found to be 6.29±0.94 mb and the total charge exchange cross section between 0° and 90° is 28.4±3.8 mb. The latter is about one-half the plane wave estimate and in good agreement with extrapolations in proton number from other nuclei.

ACKNOWLEDGMENTS

The data for this experiment were taken during the first major experimental use of the LAMPF π^0 spectrometer. Bringing such a complex instrument into operation requires the talents of many people. We wish to express our appreciation to all who helped, but especially to V. Armijo, R. Bolton, J. Cordova, C. Dalton, R. Damjanovich, D. Gallegos, R. Garcia, V. Hart, S. Johnson, G. Krausse, T. Lopez, J. Potter, J. Salas, J. Sandoval, R. Schamaun, W. Simms, C. Smith, W. Thorn, E. Weiler, and C. Welch. In addition, we wish to thank R. R. Whitney and J. S. McCarthy for the loan of the ^{3}He target. Special thanks are in order to J. Novak and N. Hoffman for helping us to operate the target. This work was supported by the United States Department of Energy. The collaborators from Tel Aviv University were supported under a grant from the United States–Israel Binational Science Foundation (BSF), Jerusalem, Israel. One of us (J.P.) was supported by the Swiss Institute of Nuclear Physics (SIN).

---

*Present address: Institut de Physique, Université de Neuchâtel, CH-2000, Neuchâtel, Switzerland.
†Present address: 30/10 Ezra Street, Rehovot 76201, Israel.
‡Deceased.
§Present address: Contraves (AG), Zürich, Switzerland.

[1]H. W. Baer, R. D. Bolton, J. D. Bowman, M. D. Cooper, F. H. Cverna, R. H. Heffner, C. M. Hoffman, N. S. P. King, J. Piffaretti, J. Alster, A. Doron, S. Gilad, M. Moinester, P. R. Bevington, and E. Winkelmann, Nucl. Instrum. Methods 180, 445 (1981).
[2]W. J. Gerace, J. P. Mestre, J. F. Walker, and D. A. Sparrow, Phys. Rev. C 22, 1197 (1980).
[3]R. H. Landau, Phys. Rev. C 15, 2127 (1977).
[4]A. T. Hess and B. F. Gibson, Phys. Rev. C 13, 749 (1976); B. F. Gibson, private communication.
[5]V. Perez-Mendez and A. W. Stetz, LAMPF Progress Report LA-8456-PR (1980), p. 66.
[6]T. J. Bowles, D. F. Geesaman, R. J. Holt, H. E. Jackson, J. Julien, R. M. Laszewski, J. R. Specht, E. J. Stephenson, R. P. Redwine, L. L. Rutledge, Jr., R. R. Segal, and M. A. Yates, Phys. Rev. C 23, 439 (1981).
[7]Y. Shamai, J. Alster, D. Ashery, S. Cochavi, M. A. Moinester, A. I. Yavin, E. D. Arthur, and D. M. Drake, Phys. Rev. Lett. 36, 82 (1976).
[8]P. Glodis, H. Brandle, R. Haddock, I. Kostoulas, N. Matz, B. Nefkens, W. Plumlee, O. Sander, J. Pratt, R. Sherman, F. Shively, and J. Spencer, Phys. Rev. Lett. 44, 234 (1980).
[9]J. Källne, H. A. Thiessen, C. L. Morris, S. L. Verbeck, M. J. Devereaux, G. R. Burleson, J. S. McCarthy, R. R. Whitney, J. R. Bolger, C. F. Moore, and C. A. Goulding, Phys. Rev. Lett. 42, 159 (1979).
[10]H. W. Baer, J. D. Bowman, M. D. Cooper, F. H. Cverna, C. M. Hoffman, M. B. Johnson, N. S. P. King, J. Piffaretti, E. R. Siciliano, J. Alster, A. Doron, S. Gilad, M. Moinester, P. R. Bevington, and E. Winkelmann, Phys. Rev. Lett. 45, 982 (1980).
[11]J. S. McCarthy, I. Sick, and R. R. Whitney, Phys. Rev. C 15, 1396 (1977).
[12]P. Y. Bertin, B. Coupat, A. Hivemat, D. B. Isabelle, J. Duclos, A. Gerard, J. Miller, J. Morgenstern, J. Picard, P. Vemis, and R. Powers, Nucl. Phys. B106, 341 (1976).
[13]R. D. Bolton, H. W. Baer, J. D. Bowman, and L. Gordon, Nucl. Instrum. Methods 174, 411 (1980).
[14]D. C. Dodder, private communication; G. Höhler, F. Kaiser, R. Koch, and E. Pietarinen, *Handbook of Pion-Nucleon Scattering* (Fack-Informations Zentrum, Karlsruhe, 1979).
[15]Following a suggestion by M. Hynes (unpublished); P. R. Bevington, *Data Reduction and Error Analysis for the Physical Sciences* (McGraw-Hill, New York, 1969), p. 111.
[16]P. R. Bevington, *Data Reduction and Error Analysis for the Physical Sciences* (McGraw-Hill, New York, 1969), p. 249.
[17]C. R. Heimbach, D. R. Lehman, and J. S. O'Connell, Phys. Rev. C 16, 2155 (1977).
[18]D. A. Sparrow, Phys. Lett. 58B, 309 (1975).
[19]J. D. Bowman, Nucl. Phys. A335, 375 (1980).
[20]K. P. Lohs and V. B. Mandelzweig, Z. Phys. A 283, 51 (1977); V. B. Mandelzweig, private communication.
[21]J. S. Mestre, Ph.D. thesis, University of Massachusetts, 1979 (unpublished).
[22]M. Wakamatsu, Nucl. Phys. A340, 289 (1980).
[23]C. H. Q. Ingram, *Meson-Nuclear Physics—1979 (Houston)*, Proceedings of the Second International Topical Conference on Meson-Nuclear Physics (AIP, New York, 1979), p. 455.
[24]D. Ashery, I. Navon, G. Azuelos, H. K. Walter, H. J. Pfeiffer, and F. W. Schleputz, Tel Aviv University Report 836-80 (1980).
[25]G. R. Burleson, G. S. Blanpied, J. Davis, J. S. McCarthy, R. C. Minehart, C. Goulding, C. L. Morris, H. A. Thiessen, W. B. Cottingame, S. Greene, and C. F. Moore, Phys. Rev. C 21, 1452 (1980).
[26]J. H. Norem, Nucl. Phys. B33, 512 (1971).